

### Rabbit-ears hybrids, VSEPR sterics, and other orbital anachronisms

Cite this: *Chem. Educ. Res. Pract.*, 2014, 15, 417

Allen D. Clauss,<sup>†a</sup> Stephen F. Nelsen,<sup>a</sup> Mohamed Ayoub,<sup>b</sup> John W. Moore,<sup>a</sup> Clark R. Landis<sup>a</sup> and Frank Weinhold<sup>\*a</sup>

We describe the logical flaws, experimental contradictions, and unfortunate educational repercussions of common student misconceptions regarding the shapes and properties of lone pairs, inspired by overemphasis on “valence shell electron pair repulsion” (VSEPR) rationalizations in current freshman-level chemistry textbooks. VSEPR-style representations of orbital shape and size are shown to be fundamentally inconsistent with numerous lines of experimental and theoretical evidence, including quantum mechanical “symmetry” principles that are sometimes invoked in their defense. VSEPR-style conceptions thereby detract from more accurate introductory-level teaching of orbital hybridization and bonding principles, while also requiring wasteful “unlearning” as the student progresses to higher levels. We include specific suggestions for how VSEPR-style rationalizations of molecular structure can be replaced with more accurate conceptions of hybridization and its relationship to electronegativity and molecular geometry, in accordance both with Bent’s rule and the consistent features of modern wavefunctions as exhibited by natural bond orbital (NBO) analysis.

Received 15th March 2014,  
Accepted 1st June 2014

DOI: 10.1039/c4rp00057a

www.rsc.org/cerp

### Introduction

The first contact of many students of organic chemistry in the early 1960s with molecular orbital (MO) theory was through Streitwieser’s influential book (Streitwieser, 1961). It mainly covered Hückel-type calculations in which non-carbon atoms are only treated by changes of  $\alpha$  and  $\beta$  parameters. Other complicating factors – such as the existence or spatial positioning of H atoms, lone pairs, or the skeletal sigma-bonding framework – were ignored entirely. “Lone pair” is not even an entry in the book’s index.

Howard Zimmerman (1963) recognized the importance of distinguishing between the hybridized and unhybridized lone pairs at the carbonyl oxygen for understanding ketone photochemistry. He employed “circle-dot-y” notation for carbonyl groups, in which the s-rich lone pair (collinear with the CO axis) is shown as small circles, the out-of-plane  $\pi_{CO}$  electrons as a pair of dots, and the unhybridized in-plane p-type lone pair as a pair of y’s, as shown in **A**.



As pointed out by Jorgensen and Salem (1973) in their book that informed a generation of organic chemists about more realistic details of electronic orbitals:

*If we are seeking favorable intramolecular interactions between lone-pairs and other orbitals, it is absolutely necessary to consider those lone pair orbitals which have the proper local symmetry.*

Although the importance of distinguishing between lone pairs of different symmetry was clearly stated over forty years ago, the distinction appears to have been widely ignored by subsequent organic and general chemistry textbook authors. Instead, the widespread teaching of valence shell electron-pair repulsion (VSEPR) theory has fostered an unfortunate tendency to envision lone pair MOs of improper local symmetry. VSEPR was introduced by Gillespie and Nyholm (1957) as a simplified way to envision heteroatom lone pairs in molecular skeletal structure [see the historical context provided in an early pedagogical review by Gillespie (1963)]. According to VSEPR theory, two equivalent “rabbit-ears” lone pairs are directed above and below the skeletal bonding plane at approximately tetrahedral angles for disubstituted group-16 (chalcogen) atoms, and three equivalent “tripod” lone pairs are similarly directed around monosubstituted group-17 (halogen) atoms. As we emphasize below, such “equivalent” (equal-energy, tetrahedrally hybridized and oriented) depictions of lone pairs cannot be consistent with the local  $\sigma$ - $\pi$  electronic symmetry of the skeletal bonding framework.

Deliberate teaching of incorrect conceptions of lone pairs and their purported “steric demands” that must be unlearned as students progress to deeper understanding of structure and

<sup>a</sup> Department of Chemistry, University of Wisconsin, Madison, WI 53706, USA.  
E-mail: clauss@chem.wisc.edu, jwmoore@chem.wisc.edu, landis@chem.wisc.edu, weinhold@chem.wisc.edu

<sup>b</sup> Department of Chemistry, UW-Washington Co., West Bend, WI 53095, USA.  
E-mail: mohamed.ayoub@uwc.edu

<sup>†</sup> Present address: Xolve, Inc., 1600 Aspen Commons #101, Middleton, WI 53562, USA.

bonding cannot be efficient or desirable (Schreiner, 2002). Although it is widely conceded that MO theory is required for proper understanding of molecular structure and bonding, VSEPR-type textbook illustrations of lone pairs often appear in close proximity to introductory MO concepts with which they are logically and mathematically incompatible. It has been steadfastly maintained by Gillespie and others that equal-energy lone pairs are “mathematically equivalent” to the proper s-rich and pure-p lone pairs (Gillespie, 1974, 2004), but this is certainly untrue except at such low levels of theory as not to warrant serious current consideration (for mathematical aspects of this purported equivalency, see Appendix 1). Although problems with VSEPR rationalizations have been pointed out repeatedly in the chemical education literature (Walsh, 1953; Laing, 1987; Clauss and Nelsen, 2009), many textbook authors and teachers remain firmly committed to teaching rabbit-ears/VSEPR structural and steric concepts that we believe are scientifically unjustifiable.

To clarify the relationship between localized Lewis structure (lone pair/bond pair) and delocalized MO descriptions of molecular electronic structure, we make frequent use of natural bond orbitals (NBOs) (Weinhold and Landis, 2012) or the closely related natural localized molecular orbitals (NLMOs) (Reed and Weinhold, 1985); for an overview of “natural”-type orbitals, see [http://nbo6.chem.wisc.edu/webnbo\\_css.htm](http://nbo6.chem.wisc.edu/webnbo_css.htm). NBOs are a unique, ‡ intrinsic, and complete set of orthonormal orbitals that optimally express the localized Lewis-like aspect of the wavefunction and are readily obtained for arbitrary wavefunctions as well as density functional and perturbative treatments of MO or correlated type. The leading Lewis-type NBOs/NLMOs have a one-to-one mapping onto the localized structural elements of the Lewis dot diagram, allowing them to serve as ideal basis functions to re-express MOs in the language of structural chemists. The pedagogical advantages of localized NBO *vs.* delocalized MO description are described more fully in a variety of journal articles (Weinhold and Landis, 2001; Weinhold, 2012; Weinhold and Klein, 2014), web-based tutorials ([http://nbo6.chem.wisc.edu/tut\\_cmo.htm](http://nbo6.chem.wisc.edu/tut_cmo.htm)), and monographs (Weinhold and Landis, 2005, 2012). Ready availability of *WebMO* (<http://www.webmo.net/>) and other web-based computational utilities (*e.g.*, <http://www.youtube.com/watch?v=Hzpr74WbDPo>) makes calculation and visualization of these orbitals increasingly practical for laptop-toting students in the modern wi-fi classroom or laboratory (see, *e.g.*, <https://www.chem.wisc.edu/content/experiment-5-computational-molecular-modeling-webmo>).

‡ As noted below, the choice of “MOs” can be rather arbitrary, insofar as *any* unitary transformation of MOs leads to the same single-determinant wavefunction with *no* effect on the energy or other observable properties of the system. MOs therefore provide no criterion for which unitarily-equivalent set is considered “best,” because all satisfy the full double-occupancy condition. In contrast, NBOs are *uniquely* determined by the form of the wavefunction (whether of MO or more complex form) because each Lewis-type NBO generally has *distinct* occupancy (<2), reflecting the fact that *some* occupancy must appear in non-Lewis NBOs to represent the physical effects of resonance-type delocalizations. The fundamental maximum-occupancy criterion of all “natural”-type methods therefore dictates uniquely which choice of NBOs is optimal, and by how much. Moreover, these NBOs are found to converge rapidly to unique limiting forms as the wavefunction approaches exactness.

## Are the lone pairs of water “equivalent”?

As described in Appendix 1, the idea that VSEPR-type lone pairs are “mathematically equivalent” to distinct s-rich and pure-p lone pairs of water rests on superficial understanding of Fock’s theorem (Fock, 1930) concerning the unitary equivalence of doubly-occupied localized (LMOs) *vs.* canonical MOs (CMOs) in single-determinant Hartree–Fock (HF) or density functional (DFT) approximations. However, at any reasonable level of MO theory, the lone pair MOs of water (whether of canonical or optimally localized NLMO form) are found to be quite *distinct* and *inequivalent*, both in form and energy. Whether one can find *some* unitary mixture of lone-pair MOs that gives resulting equal-energy orbitals is essentially irrelevant. Indeed, one could equally well find such an equal-energy mixture of core and valence-type MOs, but this provides no real justification for claiming that core and valence orbitals are somehow “equivalent.”

Fig. 1 displays 3-d surface plots of lone-pair-type MOs for H<sub>2</sub>O at diverse DFT, HF, and semi-empirical levels, illustrating their essential visual similarity to MO images of Jorgensen and Salem (1973) and *dissimilarity* to VSEPR-style cartoon images. The selected DFT and HF levels span a wide range of accuracy for treating details of chemical interactions, but *all* concur on such qualitatively important features as the inequivalent shapes and energetics of lone pairs.

Fig. 2 shows additional radial and angular details of MO *vs.* NBO lone pairs in 2-d contour plots for H<sub>2</sub>O, comparing lone pair-type MOs (Fig. 2a) with the uniquely determined s-rich ( $n_{\sigma}^{(s)}$ ) and pure-p ( $n_{\pi}^{(p)}$ ) lone-pair NBOs (Fig. 2b) at each level. The essential differences in lone pair hybridization are seen most clearly in the NBO plots, whereas MOs tend to form somewhat confusing mixtures of 1-center lone pair orbitals with symmetry-adapted combinations from other centers, as discussed below.

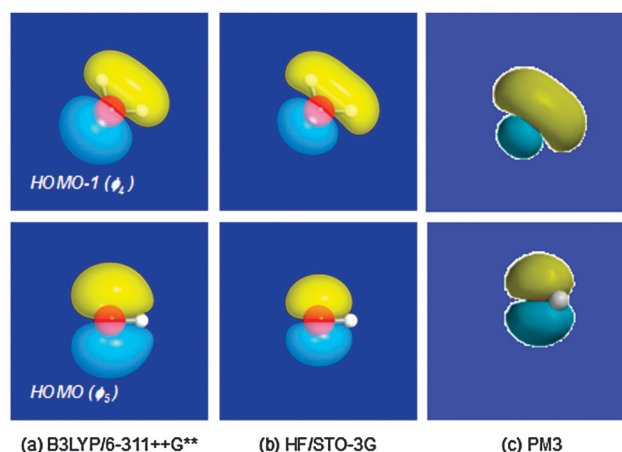


Fig. 1 Highest occupied (lone pair-like) MOs of water at various DFT, Hartree–Fock, and semi-empirical MO levels (as labeled), showing distinct  $\sigma$ -type ( $\varphi_4$ ) and  $\pi$ -type ( $\varphi_5$ ) orientation and shape at each level: (a) hybrid density functional (B3LYP) method at augmented triple-zeta basis level; (b) Hartree–Fock at minimal basis level; (c) semi-empirical “PM3” model of Dewar type. See Foresman and Frisch (1996) for more complete description of methods and basis sets used herein.

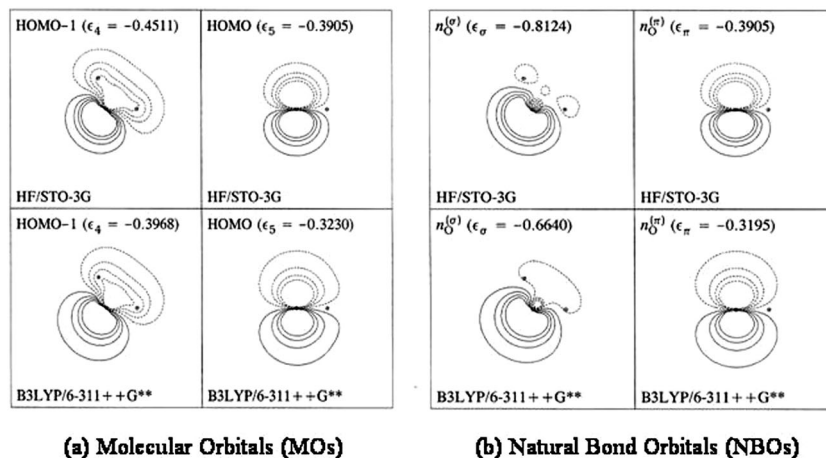


Fig. 2 2-d contour plots comparing (a) MOs and (b) NBOs for lone pairs of water at HF/STO-3G and B3LYP/6-311++G\*\* levels, showing strong inequivalencies of hybridization, energy and shape. The chosen contour plane lies within (for  $\sigma$ -type orbitals) or perpendicular to (for  $\pi$ -type orbitals) the plane of nuclei marked by crosshairs.

Mathematically and group theoretically, one can easily see (Weinhold and Landis, 2005, p. 52ff) that atomic  $s$ - $p$  symmetries can only be broken by chemical bonding interactions, and these cannot involve  $p$ -orbitals outside the line (for diatomics) or plane (for triatomics) of chemical bonding. Thus for  $\text{H}_2\text{O}$ , the pure  $p_z$  (out-of-plane) lone pair must always remain distinct from the  $s$ -rich hybridized lone pair in the  $xy$ -plane of skeletal bonding. The CMOs, NBOs, or NLMOs of  $\text{H}_2\text{O}$  must therefore exhibit the strict  $\sigma/\pi$  separation (as irreducible representations of  $C_{2v}$  symmetry) that distinguishes the unhybridized  $\pi$ -type  $n_{\text{O}}^{(\pi)}$  (pure  $p_z$ ) lone pair from the hybridized  $\sigma$ -type  $n_{\text{O}}^{(\sigma)}$  ( $\sim sp^2$ ) lone pair in the molecular plane. Even if the in-plane  $n_{\text{O}}^{(\sigma)}$  were to unaccountably lose all  $s$ -character, in gross violation of Bent's rule (Bent, 1961), the orientations and energies of  $n_{\text{O}}^{(\sigma)}$ ,  $n_{\text{O}}^{(\pi)}$  must still differ *qualitatively* from those of VSEPR-style rabbit ears.

As Fock's theorem suggests, slightly different CMO mixings may be manifested by different levels of MO theory, such as the low-level HF/STO-3G (minimal basis HF) and higher-level B3LYP/6-311++G\*\* (extended-basis DFT) levels displayed in Fig. 2. This confuses the issue slightly, because the delocalized HOMO - 1  $\phi_4$  will contain somewhat different unitary mixtures of the  $n_{\text{O}}^{(\sigma)}$  lone-pair NBO with the in-phase combination of  $\sigma_{\text{OH}}$ ,  $\sigma_{\text{OH}'}$  bond NBOs. For the MOs of Fig. 2, these mixtures are given by

$$\phi_4 = 0.79n_{\text{O}}^{(\sigma)} + 0.43(\sigma_{\text{OH}} + \sigma_{\text{OH}'}) + \dots \quad (\text{HF/STO-3G}) \quad (1a)$$

$$\phi_4 = 0.86n_{\text{O}}^{(\sigma)} + 0.36(\sigma_{\text{OH}} + \sigma_{\text{OH}'}) + \dots \quad (\text{B3LYP/6-311++G**}) \quad (1b)$$

corresponding to 62% vs. 74% lone-pair character for HF/STO-3G vs. B3LYP/6-311++G\*\*, respectively. However, as shown in Fig. 2, the energies and shapes of underlying  $n_{\text{O}}^{(\sigma)}$ ,  $n_{\text{O}}^{(\pi)}$  NBOs are quite distinct at each level and highly transferable from one level to another. These numerical examples make it clear, consistent with the group-theoretical arguments of the preceding paragraph and mathematical analysis given in Appendix 1, that

$n_{\text{O}}^{(\sigma)}$ ,  $n_{\text{O}}^{(\pi)}$  lone pairs cannot exhibit VSEPR-type "equivalency" at *any* theoretical level of useful chemical accuracy. §

## Does the local symmetry of inequivalent lone pairs persist in larger molecules?

Although the inequivalency of  $n_{\text{O}}^{(\sigma)}$ ,  $n_{\text{O}}^{(\pi)}$  lone pairs is dictated by strict triatomic  $C_{2v}$  symmetry in water, one might question whether similar  $\sigma/\pi$  separation ("effective" local symmetry) is manifested in larger molecules. Many examples might be cited to demonstrate that this is generally so. Here we briefly mention three representative organic compounds containing disubstituted oxygen whose structural/reactive properties support the (computationally unambiguous) picture of inequivalent  $n_{\text{O}}^{(\sigma)}$ ,  $n_{\text{O}}^{(\pi)}$  oxygen lone pairs and rule out conflicting VSEPR/rabbit-ears conceptions.

Fig. 3 compares 3-d visual images of the oxygen lone pair NBOs of water with those of methanol, formic acid, and furan, all at B3LYP/6-311++G\*\* level. The visual orbital images appear virtually indistinguishable, confirming the high transferability of  $n_{\text{O}}^{(\sigma)}$ ,  $n_{\text{O}}^{(\pi)}$  local-symmetry NBOs into larger species.

Table 1 displays the explicit mathematical relationships between MOs and NBOs [analogous to eqn (1a) and (1b) for water] for the alternative  $\text{CH}_3\text{OH}$ ,  $\text{HCOOH}$ , and furan species of Fig. 3. As the table shows, the high-lying MOs exhibit somewhat different mixings of intrinsic lone pair and bond NBOs in each species, but despite such confusing mixing (of no physical consequence), the MOs of highest lone-pair parentage all exhibit  $n_{\text{O}}^{(\sigma)}$ ,  $n_{\text{O}}^{(\pi)}$ -type inequivalencies similar to those of

§ Note that this remark extends also to multi-configurational GVB (Generalized Valence Bond) wavefunctions, which (even if employing rabbit-ear orbitals as initial guesses) are also found to converge self-consistently to lone-pair NBOs of clearly *inequivalent* form, similar to those of other methods discussed above.

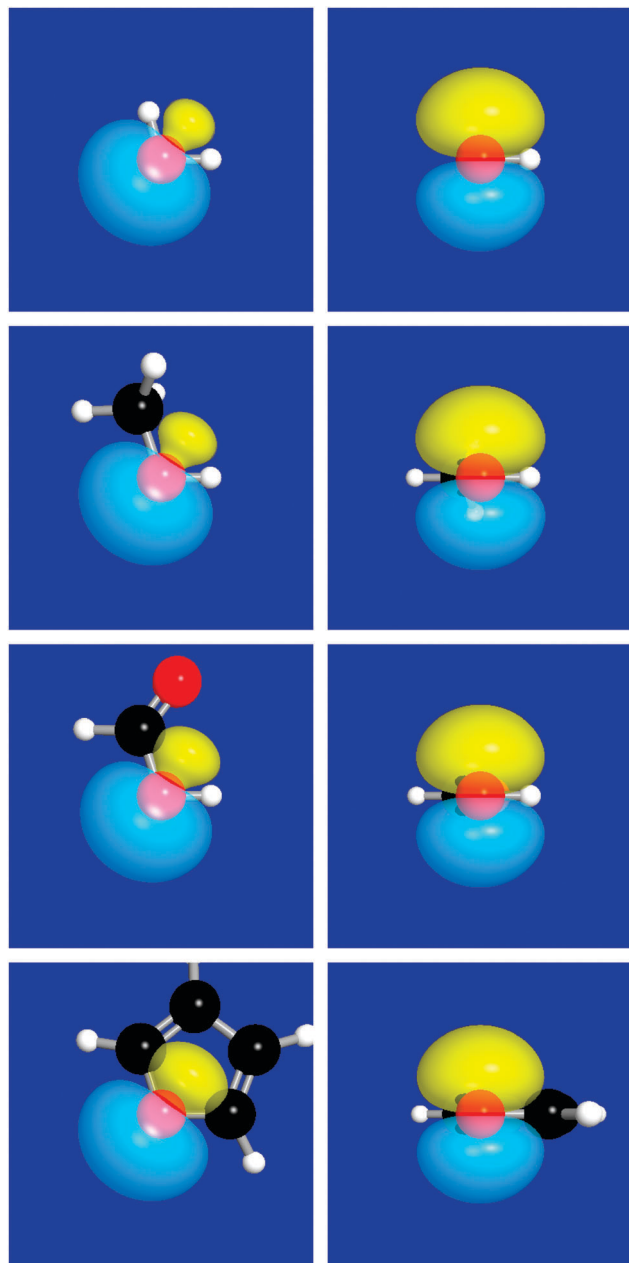


Fig. 3 3-d surface plots of  $n_{\text{O}}^{(\sigma)}$  (left),  $n_{\text{O}}^{(\pi)}$  (right) lone pairs for (from top to bottom): (a) water, (b) methanol, (c) formic acid, and (d) furan (B3LYP/6-311++G\*\* level).

Fig. 1 and 2. Thus, computational results for larger molecules consistently confirm the strong tendency to preserve effective local  $n_{\text{O}}^{(\sigma)}$ ,  $n_{\text{O}}^{(\pi)}$  ( $C_{2v}$ -like) character in all such species.

## What does experimental evidence tell us about lone pairs?

Aside from the clear computational picture, the characteristics of lone pairs can also be inferred from experimental evidence concerning their observed effects on molecular properties. Many contradictions are encountered in attempts to apply VSEPR-style

Table 1 NBO composition of “most lone pair-like” MOs (from CMO keyword option) in methanol, formic acid, and furan [cf. text eqn (1b) for water], showing leading mixings with parent  $n_{\text{O}}^{(\sigma)}$ ,  $n_{\text{O}}^{(\pi)}$  NBOs

Species	MO	NBO composition
CH <sub>3</sub> OH	$\varphi_8$	$0.68n_{\text{O}}^{(\sigma)} - 0.43\sigma_{\text{CH}} - 0.33\sigma_{\text{OH}} + \dots$
	$\varphi_9$	$0.89n_{\text{O}}^{(\pi)} + 0.32(\sigma_{\text{CH}'} - \sigma_{\text{CH}''}) + \dots$
HCOOH	$\varphi_{10}$	$0.64n_{\text{O}}^{(\sigma)} - 0.47n_{\text{O}}^{(\pi)} - 0.36\sigma_{\text{CH}} + \dots$
	$\varphi_{11}$	$0.71n_{\text{O}}^{(\pi)} - 0.67\pi_{\text{CO}'} + \dots$
Furan	$\varphi_{12}$	$0.80n_{\text{O}}^{(\pi)} + 0.41(\sigma_{\text{C}(4)\text{C}(7)} + \dots$
	$\varphi_{15}$	$0.60n_{\text{O}}^{(\sigma)} - 0.43(\sigma_{\text{C}(3)\text{H}} + \sigma_{\text{C}(4)\text{H}}) - 0.39(\sigma_{\text{C}(3)\text{C}(4)} + \dots$

reasoning to rationalize experimental properties of known compounds containing disubstituted oxygen or sulfur, examples of which will be summarized in this section.

One well-known “textbook example” is provided by the dipole analysis of hydroxylamine conformers by Jones *et al.* (1974). These workers measured the dipole moment of trimethylhydroxylamine to be 0.88 Debye and attempted to analyze its rotameric conformations about the NO bond by the VSEPR-inspired rabbit-ear lone pair analysis as shown in Fig. 4. Using simple bond-dipole additivity relationships based on other known compounds (because this was still at a time when organic chemists could not routinely perform the required electronic structure calculations!), these workers estimated the dipole moments for conformers **B**, **C**, and **D**, as shown in the figure. Because the observed dipole moment was less than that estimated for the staggered structures **C** and **D**, they concluded that eclipsed structure **B** must be present. Because **C** has “large” lone pairs crowded together, its contribution was neglected, and the molecule was concluded to be approximately a 3 : 1 mixture of **D** : **B**.

However, this conclusion is fundamentally incorrect (Nelsen *et al.*, 1987), and the error can be traced to the rabbit-ear lone pair representation that was used. Similar analysis using the proper  $n_{\text{O}}^{(\sigma)}$  and  $n_{\text{O}}^{(\pi)}$  lone pairs is shown in Fig. 5. **B** and **C** are energy minima, but **B** is no longer “eclipsed,” and **D** (selected as the most important contributor by rabbit-ears analysis) is not even an energy minimum! (Even semi-empirical calculations get this right, because they use proper lone pairs.) As shown more clearly in the first figure of Riddell (1981) review of hydroxylamine geometries, **D** lies on the side of a hill on the energy surface for ON rotation, so it cannot be contributing to the observed dipole moment because no significant amount is present. The s-rich lone pairs are shown close to oxygen in Fig. 5, because they are so compact and low in energy as to have no significant interaction with adjacent methoxy substituents, and therefore make no significant contribution to the torsional energy surface.

Still more striking experimental contradictions to VSEPR-inspired rabbit-ears conceptions are provided by sulfur compounds, including the ubiquitous CSSC disulfide structural motifs of proteins and peptides. Early structural understanding of such species came from electron diffraction measurements on HSSH (Winnewisser *et al.*, 1968; Hahn *et al.*, 1991), MeSSMe (Sutter *et al.*, 1965; Beagley and McAloon, 1971; Yokozeki and

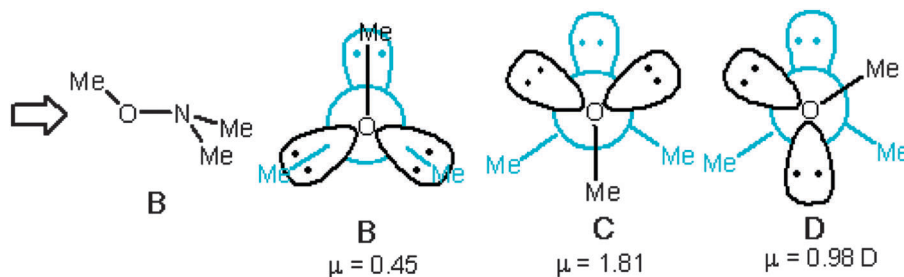


Fig. 4 VSEPR-type rabbit-ears cartoons for trimethylhydroxylamine conformers in Newman projections (with arrow showing view direction, and rear NMe<sub>2</sub> group in light blue).

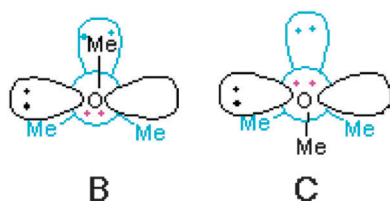


Fig. 5 Similar to Fig. 4, for proper p-rich (black lobes) and s-rich (magenta dots) lone pairs at oxygen.

Bauer, 1976), ClSSCl (Beagley *et al.*, 1969; Kniep *et al.*, 1983), and FSSF (Kuczkowski, 1964; Marsden *et al.*, 1989), but because organic and biochemists were unfamiliar with such techniques, the significance of the work was too long overlooked. Here again the use of rabbit-ears lone pairs leads to misunderstanding. As shown in Fig. 6, the VSEPR-inspired view of disulfide linkages (with each sulfur bearing “bulky” rabbit-ears lone pairs at tetrahedral angles) would lead to the expectation of XSSX dihedral angle  $\theta = 180^\circ$ , to minimize “steric clashes” between lone pairs. Alternatively, if anomeric  $n_S-\sigma^*_{SH}$  interactions are judged most important, the tetrahedral rabbit-ears orientation predicts a preferred  $\theta \cong 60^\circ$  conformation. However, neither expectation is correct! The preferred  $\theta$  is found to be near  $90^\circ$  for all the above examples (as the inequivalent  $n_S^{(\sigma)}$ ,  $n_S^{(\pi)}$  model suggests), and the correct result is calculated even by simple semi-empirical methods that incorporate the necessary lone pair inequivalencies originally pointed out by Jorgensen and Salem (1973).

The disulfide species are also instructive with regard to the seemingly unending debates about steric *vs.* hyperconjugative effects in torsional phenomena (Bickelhaupt and Baerends, 2003; Weinhold, 2003). It had been common (Steudel, 1975) to rationalize the  $\theta \cong 90^\circ$  conformational preference of disulfides

in terms of a “4e-repulsive” interaction between vicinal  $n_S^{(\pi)}$  lone pairs. However, structural data strongly suggest that the  $90^\circ$  preference arises because the high-energy pure-p  $n_S^{(\pi)}$  lone pair is thereby able to align most favorably with vicinal  $\sigma^*_{SH}$  acceptor orbitals for maximal  $n_S^{(\pi)}-\sigma^*_{SH}$  hyperconjugative stabilization. If the hyperconjugative model is correct, one ought to see characteristic SS bond length variations reflecting  $n_S^{(\sigma)}-\sigma^*_{SX}$  attraction, and therefore sensitive to *X electronegativity* (rather than “steric bulk”) variations. This is indeed found to be the case, with experimental SS bond lengths of 2.056 Å for HSSH, 2.029 Å for MeSSMe, 1.943 Å for ClSSCl, and 1.890 Å for FSSF. Similar resolutions of steric *vs.* hyperconjugative controversies are found for hydrazines (Petillo and Lerner, 1993), peroxides (Carpenter and Weinhold, 1988), and numerous other species (Pophristic and Goodman, 2001).

## Other pedagogical dilemmas of using VSEPR-derived lone pairs

As known from many studies of stereochemical and anomeric phenomena (Delongchamps, 1983; Kirby, 1983), lone pairs commonly act as powerful electronic donors (Lewis bases) in conjugative and hyperconjugative donor–acceptor interactions. Many details of structure and reactivity are therefore *sensitive* to lone pair shape, energy, and orientation, enabling one to clearly distinguish equivalent (rabbit ears) from inequivalent ( $n_S^{(\sigma)}/n_S^{(\pi)}$ ) lone pairs. This has important implications in how we teach about lone pairs in general chemistry and introductory organic chemistry. The current common practice of using VSEPR to predict and explain electronic structure, particularly the spatial orientation of lone pair electrons, results in a need to start “unteaching” incorrect perceptions or having to use convoluted,

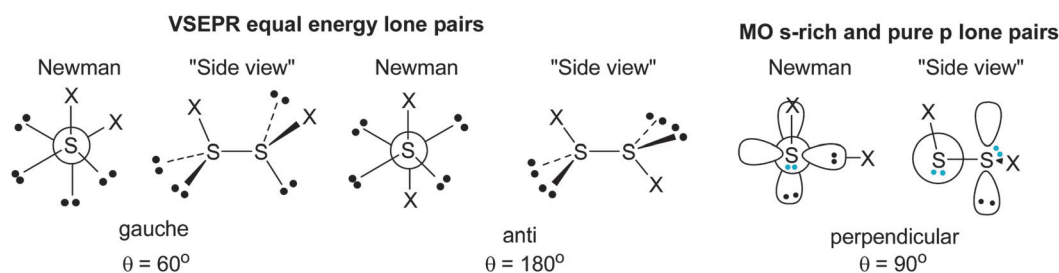
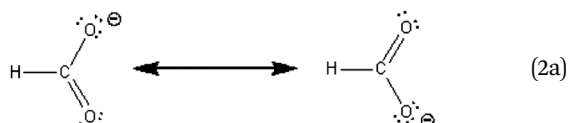


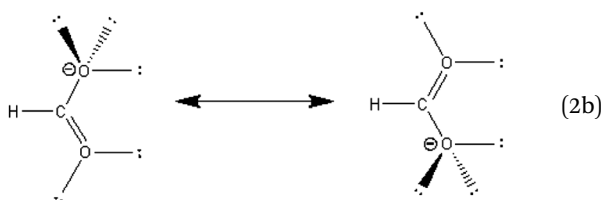
Fig. 6 Expected conformers of XSSX compounds in VSEPR (left) vs. MO (right) lone-pair formulations.

invalid rationalizations almost immediately to help students work around their incorrect perceptions about lone pairs.

In introductory organic chemistry, contradictions with VSEPR arise early when students are introduced to the concept of resonance involving oxygen or nitrogen atoms conjugated to  $\pi$  systems. The contradictions go unnoticed by some (but not all) students and are glossed over by instructors who prefer not to start unteaching VSEPR immediately after it was covered. As a result, students are taught to draw resonance structures without considering the types of orbitals involved. If they do consider the types of orbitals, it becomes apparent that they are forming  $\pi$ -bonds using  $sp^3$  orbitals. For example, when students learn about the acidity of carboxylic acids and the importance of resonance stabilization of carboxylate anions, they are taught to recognize resonance of the type shown in (2a) for the formate anion as being particularly stabilizing.



Using the VSEPR model, if students consider the orbitals involved in these resonance forms, then the lone pairs would have local symmetry as shown in (2b) which would prevent any of the lone pairs on the anionic oxygen from forming a  $\pi$ -bond to the carbon atom.



Many instructors avoid addressing this contradiction, while others refer to the anionic oxygen “rehybridizing” to  $sp^2$  allowing it to enter into resonance. Invoking such rehybridization arguments when there was no valid basis for considering the oxygen to be  $sp^3$  hybridized to begin with is clearly a pedagogically unsound practice.

Whether or not such contradictions arise when the concept of resonance is first introduced, they invariably arise some weeks later when the structure and reactivity of conjugated and aromatic compounds are discussed in greater detail. For example, when discussing aromaticity, furan ( $C_4H_4O$ ) is commonly cited as a heterocyclic compound that exhibits the classical chemical characteristics of aromaticity (Katritzky and Lagowski, 1967). However, students trained to use VSEPR consider the oxygen lone pairs in furan to be in equivalent  $sp^3$  orbitals projecting above and below the plane of the ring as shown in (3),



which leads them to the logical conclusion that furan should not be aromatic because neither lone pair can be part of the  $\pi$  system of the

ring. (If instead the rabbit-ears lone pairs are both counted as belonging to the  $\pi$  system, the usual  $4n + 2$  rule for aromaticity is again violated.) Many such conflicts can only be glossed over by inattention to orbital details.

Numerous related organic chemistry examples could be cited where VSEPR-inspired thinking leads to contradictions and incorrect conclusions. Indeed, most conjugated systems containing heteroatoms tend to be viewed incorrectly by students trained to use VSEPR, resulting in a range of incorrect perceptions about the structure, stability, and reactivity of these systems. By the time students have completed one semester of introductory organic chemistry, they have encountered so many of these examples that their use of VSEPR to predict and explain electronic structure hurts their understanding more often than it helps.

Still other pedagogical dilemmas are presented by the VSEPR-inspired concept that lone pairs are sterically “repulsive” compared to bond pairs. Gillespie (1963) recommended teaching that the tetrahedral hydride bond angles of methane were reduced to observed values in ammonia ( $107.3^\circ$ ) and water ( $104.5^\circ$ ) because:

[lone pairs] overlap with neighboring orbitals more extensively and therefore will repel electrons in these neighboring orbitals more strongly than an electron pair in a bonding orbital [with the result that] lone pair electrons will tend to move apart and squash bonding electron pairs together

Such language leads to the widespread perception that lone pairs are somehow “effectively bigger” than bonding electron pairs. However, we may well ask what evidence (other than mnemonic success of the VSEPR model itself) supports the claim that lone pairs are effectively “bigger,” “more repulsive,” or “sterically demanding” compared to bond pairs, or the assumption that moving lone pair electrons apart (*i.e.*, in the orthogonal  $xz$ -plane) should “squash” the  $\sigma_{OH}$  hydride bonds to reduced angle in the molecular  $xy$ -plane of water.

On the experimental side, organic chemists often assess the relative size of substituents by determining the equilibrium constant and Gibbs free energy difference between the axial and equatorial conformers of a six-membered ring containing the substituent (Anslyn and Dougherty, 2006). For any substituent larger than a hydride bond, the conformation that places the bulky substituent in the equatorial position is expected to be lower in energy, due to the unfavorable non-bonded 1,3 diaxial interactions with CH bonds that occur when the substituent is in the axial position. As shown in Fig. 7, this method can be applied to piperidine ( $C_5H_{10}NH$ ) to assess the effective size of the nitrogen lone pair relative to the  $\sigma_{NH}$  hydride bond. Fig. 7 displays the experimental Gibbs free energy difference, + 0.36 kcal mol<sup>-1</sup> (Anet and Yavari, 1977), which demonstrates

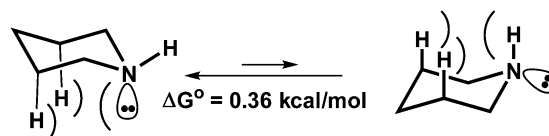


Fig. 7 Gibbs free energy difference for axial vs. equatorial isomers of piperidine, indicating that the lone pair is effectively smaller than the hydride bond pair at nitrogen.

**Table 2** Hybridization parameter ( $0 \leq \lambda \leq \infty$ ), percentage s/p-character, and associated bond angle for representative  $sp^2$  hybrids [cf. eqn (4)–(6)]

Type	$\lambda$	%-s	%-p	$sp^2$ - $sp^2$ angle
Pure s	0	100.0	0.0	(Isotropic)
sp	1	50.0	50.0	180.0°
$sp^2$	2	33.3	66.7	120.0°
$sp^3$	3	25.0	75.0	109.5°
$sp^{3.5}$	3.5	22.2	77.8	106.6°
Pure p	$\infty$	0.0	100.0	90.0°

that the  $n_N$  lone pair of piperidine definitely prefers the *axial* position, and thus appears *smaller* than the  $\sigma_{NH}$  hydride bond by this experimental criterion.¶ Such experimental conflicts with VSEPR expectations become increasingly numerous and troublesome as the student progresses to more advanced levels.

## How can one satisfactorily explain X–O–Y bond angles without VSEPR?

As recognized by Pauling (1931), Slater (1931), Coulson (1961), and others, the basic origins of near-tetrahedral bond angles in main-group bonding lie in the *hybridization* concept. The subtle variations from tetrahedrality are similarly due to the subtle variations of hybridization (and therefore bond angle) with *electronegativity*, as expressed most succinctly in Bent's rule (Bent, 1961), *viz.*:

*Central main-group atoms tend to direct bonding hybrids of higher p-character toward atoms of higher electronegativity*

With this powerful mnemonic in hand, the student can easily employ elementary concepts of Lewis structure, periodic electronegativity trends, and bond hybrid vs. angle relationships to make VSEPR-style predictions of molecular structure with confidence and accuracy.

The fundamental relationship between main-group hybrids [e.g., hybrids  $sp^{\lambda_i}$ ,  $sp^{\lambda_j}$  (with hybridization parameters  $\lambda_i$ ,  $\lambda_j$ ) to atoms  $i$ ,  $j$ ] and bond angle  $\theta_{ij}$  is given by Coulson's (1961) directionality theorem (Weinhold and Landis, 2005, p. 110ff),

$$\cos(\theta_{ij}) = -(\lambda_i \lambda_j)^{-1/2} \quad (4)$$

which should be known to every chemistry student. Each hybrid parameter  $\lambda$  is merely a convenient way of expressing the percentage p-character of the hybrid, *viz.*

$$\lambda = (\%p)/(\%s) \quad (5)$$

which might vary as shown in Table 2 from 0–100% (or any value in between). Because only three p orbitals and one s orbital comprise the atomic valence shell, the four valence hybrid  $\lambda_i$ 's must satisfy the conservation law

$$\sum_{i=1-4} 1/(1 + \lambda_i) = 1 \quad (\text{conserve s-character}) \quad (6a)$$

¶ It should be noted that experimental cyclohexane A-factors may also involve significant axial-equatorial differences in hyperconjugation, so they appear to be less reliable measures of “pure” steric effects than other theoretical criteria described below.

or equivalently

$$\sum_{i=1-4} \lambda_i/(1 + \lambda_i) = 3 \quad (\text{conserve p-character}) \quad (6b)$$

Each conservation law (6a) and (6b) makes clear that increasing the electronegativity of any ligand (thereby increasing  $\lambda_i$ , according to Bent's rule) must necessarily *reduce* the p-character in other hybrids, and thereby alter the bond angles according to eqn (4). This is simply how hybridization (orbital mixing) works, with no “squashing” required. The simple hybrid/angle eqn (4)–(6) allow one to trump VSEPR theory by predicting not only the *direction* but also the approximate *magnitude* of angular change.

Consider, for example, replacement of methane ( $CH_4$ ) by substituted  $CH_3X$ . According to Bent's rule, the equivalent  $sp^3$  hybrids of methane (each with 75% p-character) must then be replaced by *inequivalent* hybrids (with  $\lambda_H \neq \lambda_X$ , to reflect the inequivalent bonding demands of H and X ligands) subject to the conservation constraint (6b),

$$3\lambda_H/(1 + \lambda_H) + \lambda_X/(1 + \lambda_X) = 3 \quad (7a)$$

which can be solved to give

$$\lambda_H = 2 + 3/\lambda_X \quad (7b)$$

The altered  $\lambda_X$ ,  $\lambda_H$  values can then be substituted in eqn (4) to obtain estimated  $\theta_{HX}$  and  $\theta_{HH}$  bond angles. For example, if X is highly electronegative (e.g., X = F), its hybrid acquires *more* than 75% p-character [e.g.,  $\lambda_F = 3.65$  (78.5% p-character),  $\lambda_H = 2.79$  (73.6% p-character) in  $CH_3F$  (B3LYP/6-311++G\*\* level, idealized tetrahedral geometry)], and eqn (4) then gives

$$\theta_{HF} = \arccos[-1/(\lambda_F \lambda_H)^{1/2}] = 108.3^\circ \quad (8a)$$

$$\theta_{HH} = \arccos[-1/\lambda_H] = 111.0^\circ \quad (8b)$$

in sensible agreement with fully optimized values (108.6°, 110.3°, respectively). Approximations of  $\lambda_X$  from electronegativity values (as well as limitations of the resulting numerical estimates) are discussed elsewhere (Weinhold and Landis, 2005, pp. 138–151), but one requires only the elementary relationship (4) between bond angle  $\theta_{ij}$  and hybrid descriptors  $\lambda_i$ ,  $\lambda_j$  to see how Bent's rule predicts the direction of angular changes from familiar electronegativity differences.

Replacement of a bond pair by a lone pair is also straightforward if we think of the lone pair as bonding to a “ghost” atom X (least electronegative of all!). In  $H_2O$ , for example, we expect the in-plane lone pair to exhibit *reduced* p-character, with correspondingly higher p-character in hydride bonds [e.g.,  $\lambda_{n(\sigma)} = 0.97$  (49.3% p-character) vs.  $\lambda_H = 3.05$  (75.3% p-character)]. The predicted hybridization shifts thereby lead to bond-angle changes corresponding to “increased angular volume” around lone pairs, as suggested (for the wrong reasons) by VSEPR theory.

Indeed, with only slight changes of terminology, we can easily re-phrase the familiar VSEPR examples in more accurate and incisive hybrid language. For example, we should describe lone pairs as “s-rich” or “angularly rounded” (rather than “fat” or “more repulsive”). Of course, the temptation to envision

rabbit-ear lone pairs should never arise in the reformulated presentation, because the out-of-plane  $n_{\text{O}}^{(\pi)}$  lone pair (pure-p, with  $\lambda_{n(\pi)} = \infty$ ) is always excluded from the Bent's rule competition for in-plane p-character.

Why does Bent's rule work? Electrons of a free carbon atom will naturally prefer to remain in a low-energy s-orbital rather than high-energy p-orbital. Chemical C–X bonding can force s–p mixing (hybridization) to lower the overall energy, but the optimal s/p-composition of the C hybrid will naturally depend of how “close” the electron pair remains to the carbon atom. If X is relatively electropositive, so that the C–X bond is highly polarized toward C, the optimal C hybrid incorporates increasing s-character (and increasingly broad angular “roundness”) to minimize the energy. However, if X is electronegative, so that C–X polarization takes the electron pair away from C, the optimal C hybrid incorporates increasing p-character (and increasingly narrow angular directionality). Bent's rule can also be appropriately re-formulated for transition metal species (Weinhold and Landis, 2005, p. 421ff), where it continues to provide excellent guidance to molecular structure predictions for mononuclear and polynuclear metallic species. In contrast, VSEPR theory exhibits numerous spectacular failures in this domain (Weinhold and Landis, 2005, pp. 389, 390, 400, 402, 428, 433, 449, 454, 574).

The hybridization changes implied by Bent's rule can also be recognized in “Walsh diagrams” (Walsh, 1953) that exhibit MO (or NBO) orbital energy as a function of bond angle or other variable of interest. Fig. 8 displays the NBO-based Walsh diagrams for bond ( $\sigma_{\text{OH}}$ ) and lone pair ( $n_{\text{O}}^{(\sigma)}$ ,  $n_{\text{O}}^{(\pi)}$ ) orbitals as p-character reallocates during HOH bond-bending. As shown in Fig. 8, the energy of the in-plane  $n_{\text{O}}^{(\sigma)}$  lone pair steadily decreases at smaller HOH bond angles, reflecting its diminished p-character as

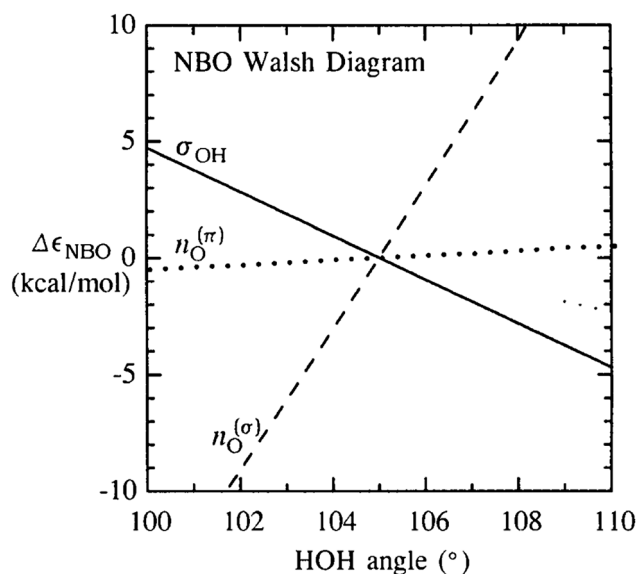


Fig. 8 NBO-based Walsh diagram (B3LYP/6-311++G\*\* level), showing NBO orbital energies for  $\sigma_{\text{OH}}$  bond (solid line),  $n_{\text{O}}^{(\sigma)}$  lone pair (dashed line), and  $n_{\text{O}}^{(\pi)}$  lone pair (heavy dotted line) as function of HOH bond angle, reflecting competing in-plane demands for p-character in accordance with Bent's rule.

required by the increased p-character (and higher orbital energy) for the two  $\sigma_{\text{OH}}$  bonds. In contrast, the out-of-plane  $n_{\text{O}}^{(\pi)}$  is scarcely affected by angular deformations, testifying to its profound inequivalence to  $n_{\text{O}}^{(\sigma)}$  with respect to the competition for p-character. Although other factors (including nuclear-nuclear repulsion and Coulomb/exchange variations) contribute to  $\Delta E_{\text{tot}}$ , the dominant orbital-energy dependence is clearly exhibited by the  $\epsilon(n_{\text{O}}^{(\sigma)})$  and  $\epsilon(\sigma_{\text{OH}})$  NBO variations in Fig. 8, as anticipated by Bent's rule.

## How can one more accurately characterize the “steric” properties of lone pairs?

Physicist Victor F. Weisskopf (1975) first proposed a visually and mathematically effective formulation of steric repulsion as “kinetic energy pressure.” Steric space-filling or “hardness” properties are generally understood to originate in the Pauli exclusion principle, which limits the maximum occupancy of any spatial orbital to two electrons of opposite spin. Equivalently, this principle prevents electron pairs from crowding into the same spatial region, because their orbitals cannot maintain mutual orthogonality without incurring additional oscillatory “ripple patterns” (nodal features) that increase the 2nd-derivative “curvature,” and thus the kinetic energy of the orbital. Attempted compression of filled orbitals must therefore result in increasingly severe ripple-like nodal features in the outer overlap region, analogous to the inner nodal features that maintain orthogonality to core electrons of the same symmetry. In each case, the increase in kinetic energy associated with such ripples acts as an opposing “pressure” to resist further compression.||

Weisskopf's picture forms the basis of *natural steric analysis* (Badenhoop and Weinhold, 1997a), a standard option of the NBO program (<http://nbo6.chem.wisc.edu>) that quantifies total “steric exchange energy” ( $E_{\text{NSX}}$ ) as well as the pairwise contributions from distinct electron pairs. The  $R$ -dependent variations of  $E_{\text{NSX}}$  provide an excellent approximation for the rare-gas interaction potentials that are considered the prototype of steric exchange effects. The  $\Delta E_{\text{NSX}}(R)$  variations are also found to satisfy numerous consistency checks with empirical van der Waals radii and other physical criteria of steric size (Badenhoop and Weinhold, 1997b, 1999). We may therefore employ NBO steric analysis to directly assess the steric-exchange effects with respect to HOH bond-angle variations, as plotted in Fig. 9. The figure shows that increasing the HOH angle always causes the overall  $E_{\text{NSX}}$  steric repulsions to decrease, contrary to the lone

|| Why orbitals must remain mutually orthogonal, and why the curvature of orbital ripple patterns determines kinetic energy, goes back to deep quantum mechanical principles. However, the idea (as epitomized, e.g., in the Bohr relationship  $E = h\nu$ ) that increased number of oscillatory nodes corresponds to unfavorable increase in energy should be familiar to all students. Chemistry students learn the value of using the visual overlap of idealized free-atom orbitals to estimate orbital interaction strength. However, one should recognize that pre-NBOs and other such “visualization orbitals” are merely a convenient mnemonic, whereas the physical solutions of Schrödinger-type eigenvalue equations, as well as the associated perturbation theory equations, are always mutually orthogonal (Weinhold, 2003), consistent with Weisskopf's formulation of the steric concept.



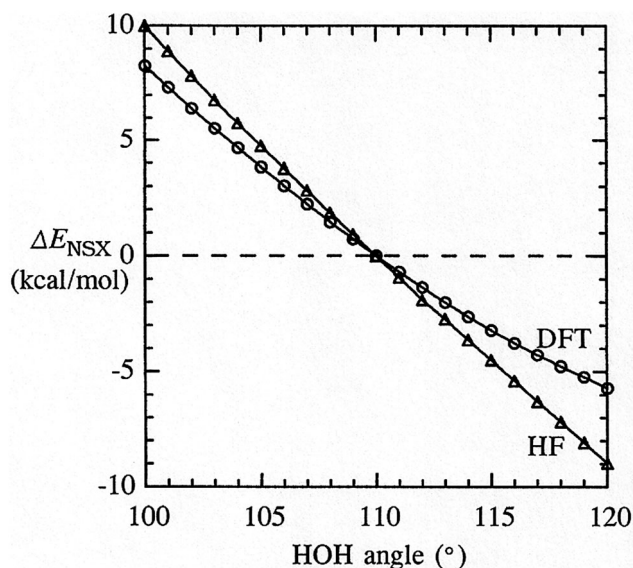


Fig. 9 Natural steric-exchange energy variations ( $\Delta E_{\text{NSX}}$ ) with  $\text{H}_2\text{O}$  bond angle (referenced to  $110^\circ$ ), showing the uniform decrease of steric repulsion toward smaller HOH angles, contrary to expectations of VSEPR theory. Similar trends are found for HF/STO-3G (triangles) and B3LYP/6-311++G\*\* (circles) levels of theory.

pair “squashing” that would be expected in VSEPR theory. Various levels of HF or DFT theory differ slightly in overall slope and individual orbital contributions, but *no* reasonable theoretical level provides support for “VSEPR sterics” as presented in current chemistry textbooks.

An even simpler way to assess relative lone-pair *vs.* bond-pair “steric size” is by plotting realistic  $n_{\text{O}}^{(\sigma)}$ ,  $\sigma_{\text{OH}}$  orbital shapes. (Recall that the orthogonal  $n_{\text{O}}^{(\pi)}$  lone pair makes no contribution to sterics in the molecular plane.) Bader *et al.* (1967) proposed the outermost contour value 0.0316 a.u. as closely approximating the effective van der Waals boundary inferred from crystallographic data. With this contour value, Fig. 10 compares the apparent orbital sizes for lone-pair *vs.* bond-pair NBOs in 1-d orbital amplitude (left) and 2-d contour (right) plots for water.

As shown in these plots, one can visually judge that the lone pair appears everywhere “sterically hidden” or “inside” the bond pair within a broad cone of approach angles along the

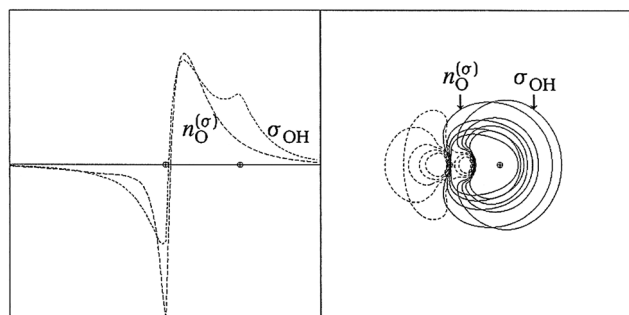


Fig. 10 Apparent “steric size” of lone pair ( $n_{\text{O}}^{(\sigma)}$ ) *vs.* bond pair ( $\sigma_{\text{OH}}$ ) NBOs of  $\text{H}_2\text{O}$  (B3LYP/6-311++G\*\* level), compared in terms of 1-d orbital amplitude profiles (left) or 2-d contours (right).

forward direction. Neglecting a short-range feature on the  $n_{\text{O}}^{(\sigma)}$  backside (seldom the approach direction of chemical interest!), the  $n_{\text{O}}^{(\sigma)}$  orbital appears sterically “visible” only in a narrow (near-transverse) angular sector near the nucleus, where its “more rounded” shape is in accordance with Bent’s rule. Such simple visual comparison may have greater pedagogical impact than the  $\Delta E_{\text{NSX}}$  evaluations of Fig. 9 in establishing that superficial VSEPR-inspired steric concepts bear little or no relationship to the actual shapes and sizes of lone pair and bonding orbitals as found in modern wavefunctions.

## How can the present freshman curriculum be modified to achieve VSEPR-free concepts of directed valency and molecular shape?

A VSEPR-free introduction to hybridization and molecular shapes can be achieved with some shifts of emphasis in standard textbook presentations. As a specific pedagogical model, we consider the textbook “Chemistry: The Molecular Science” (CMS) of Moore and Stanitski (2015), where Chapters 5–7 are the respective modules on atoms (CMS-5), diatomic covalent bonding (CMS-6), and polyatomic molecular shape (CMS-7). The overall aim is to retain proper focus on the directional nature of covalent bonding and how hybridized bonding concepts are used to visualize the 3-dimensional structures of molecules, small and large. Modern molecular and orbital visualization tools enable students to begin acquiring accurate visual perceptions of orbital shapes and the maximum-overlap principles that govern molecule construction, long before the underlying details of quantum mechanics and computational technology need to be confronted.

Specifically, the modified CMS-5 module should develop the concept of atomic orbitals (AOs) and *phase*, using a variety of dot-density and surface diagrams to convey radial and angular features of hydrogenic ground and excited-state atomic orbitals, including the oscillatory sign variations that are needed to keep s, p, d orbitals properly independent (orthogonal) as distinct excitation states. The CMS-6 module should similarly develop the *superposition* concept – the in-phase (constructive) and out-of-phase (destructive) mixing of hydrogenic 1s AOs to form the ground state “bonding” and excited state “antibonding” orbitals of diatomic species such as  $\text{H}_2^+$ ,  $\text{H}_2$ ,  $\text{He}_2^+$ , and  $\text{He}_2$ . (The restricted palette of choices allowed by the Pauli principle should also be emphasized at this point, progressively quenching opportunity for chemical bonding as one moves from  $\text{H}_2$  to  $\text{He}_2^+$  to  $\text{He}_2$ ). Students are thereby visually introduced to an important special case of the superposition principle: If an electron is offered a choice of localizing on one H atom *or* the other, quantum superposition guarantees that a *better* (in-phase, “bonding”) orbital can be found that involves *sharing* between atoms and *lowering* of energy, the essence of chemical bond formation (Weinhold, 1999).

The stage is then set for CMS-7, the introduction to polyatomic molecular structure. This module might begin with free-form “student discovery” of gas-phase covalent molecule structures with

a tool such as *Models 360* (<http://www.chemeddl.org/resources/models360/models.php?pubchem-11638>), which allows students to visually explore bond lengths, angles, and characteristic “shapes” around divalent, trivalent, or tetravalent atoms in an impressionistic manner. Such explorations can be designed for group work by assigning each member a particular atom and the task of tabulating and seeking generalizations about favored molecular bond lengths (sums of “atomic radii”?) and angles (near-trigonal or tetrahedral?), particularly the propensity to form distinctive shapes in one, two, or three dimensions.

With such empirical generalizations in hand, one can move to considering bonding of covalent hydrides in 2nd-row elements. Begin with HF, where the valence-shell building blocks of F are 2s, 2p, the former isotropic (undirected) and smaller in size, but lower in energy. If the hydrogen nucleus is located along the z axis, one can see by inspection that only the 2s and 2p<sub>z</sub> orbitals of F can have constructive bonding overlap with the 1s of H, whereas the remaining 2p<sub>x</sub> and 2p<sub>y</sub> orbitals (perpendicular to the bonding axis) must become off-axis “left-overs” for non-bonding (lone pair) electrons. With respect to the apparent alternatives available to on-axis (“active”) 2s, 2p<sub>z</sub> bonding atomic orbitals of F, the quantum superposition principle once again guarantees that some *mixture* (hybrid) of 2s, 2p<sub>z</sub> must give better overlap (and lower energy) than either “pure” alternative alone. As students can readily verify with graphical visualization tools, a 50 : 50 mixture (2s + 2p<sub>z</sub>, “sp hybrid”) gives greater directionality and overlap with the target 1s orbital on H than either 2s or 2p<sub>z</sub> alone. Such an in-phase sp-hybrid is therefore used to form the 2-center ( $\sigma_{\text{FH}}$ ) orbital for the bond pair, whereas the out-of-phase sp hybrid (oppositely directed along the z axis) and the unhybridized off-axis 2p<sub>x</sub>, 2p<sub>y</sub> orbitals contain the lone pairs of the formal Lewis structure. The on-axis sp-hybrid lone pair (with 50% s-character) is naturally quite distinct in energy and shape from the higher-energy off-axis 2p<sub>x</sub>, 2p<sub>y</sub> lone pairs, discouraging any temptation to think of equivalent (“tripod-like”) spatial distributions and chemical properties of fluoride lone pairs.

This brings us to the case of water, where the O atom has the usual 2s, 2p<sub>x</sub>, 2p<sub>y</sub>, 2p<sub>z</sub> valence orbitals and each H has the 1s orbital. As in HF, the first OH bond may be oriented along the z axis, using the in-phase (s + p<sub>z</sub>) hybrid. Will the second OH bond prefer a linear or bent geometry? If linear, the only option is to use the oppositely directed (s – p<sub>z</sub>) hybrid for the second bond pair, which leaves the remaining 2p<sub>x</sub>, 2p<sub>y</sub> orbitals for lone pairs. If bent (say, in the y–z plane of bonding), an additional 2p<sub>y</sub> orbital becomes available to participate in hybridization and bonding (*e.g.*, by forming three equivalent “sp<sup>2</sup>” hybrids, each of 33% s-character, oriented at 120° to one another) while leaving 2p<sub>x</sub> as the p-type lone pair perpendicular to the bonding plane. At this point one can introduce Coulson’s directionality theorem, to determine inter-hybrid angles for various proposed hybrid compositions, and Bent’s rule, to allocate %s vs. %p character most sensibly between bonding vs. non-bonding hybrids (or bonding partners of higher vs. lower electronegativity). The elements for discussion of general “sp<sup>2</sup>” hybridization (where  $\lambda$  is the ratio of %p to %s character) are thereby in place, and the elementary orbital reasoning underlying both Bent’s rule and the Coulson formula (4) will be seen as highly intuitive and fully

consistent with accurate orbital visualizations. One thereby achieves the desired goal of instilling more accurate conceptions of orbitals (automatically consistent with graphical displays of accurate wavefunction properties) and the deep relationships between electronegativity differences, hybrid composition, and molecular geometry, while avoiding superficial VSEPR/rabbit-ears conceptions of water lone pairs.

As a pedagogical bonus, one also has the corresponding compositions and shapes of the *antibonding* (unoccupied “non-Lewis”) partners of the final bonding orbitals, which serve as sites of potential *change* of electronic configuration. Thus, students are immediately prepared to focus on the “donors” (occupied Lewis-type orbitals) and “acceptors” (vacant non-Lewis orbitals) that lead to important donor–acceptor interactions (resonance corrections to the elementary Lewis structure picture) or the full electron *transfers* of electronic spectroscopy or chemical reaction phenomena. Appendix 2 includes a current handout for a main-line freshman chemistry course (Chem 104 at the University of Wisconsin, Madison) that illustrates the power of such “donor-acceptor thinking” in perceiving the deep relationships between molecular structure and reactivity at a surprisingly sophisticated level.

## Conclusion

The foregoing examples serve to illustrate how *qualitative* chemical misrepresentations are inspired by VSEPR concepts, and why the teaching of such concepts ought to be sharply downgraded or abandoned. Fairly simple changes in emphasis and language allow one to retain the popular molecular structural predictions of the “VSEPR module,” but to integrate (and extend!) these predictions in the framework of more accurate teaching of hybridization and Bent’s rule concepts. The latter form the basis for modern valency and bonding principles that extend successfully to main-group and transition-group species far beyond the scope of freshman chemistry. These principles are also completely consistent with (indeed, derived from and inspired by) the best available computational evidence from modern wavefunctions. They are also consistent with “bottom-up” and “active learning” strategies (Levy Nahum *et al.*, 2008; Alberts, 2013) to better integrate the problem-solving tools and techniques of modern research into the undergraduate curriculum, and they connect with other recent work (Hinze *et al.*, 2013) on the effectiveness of scientific visualization tools. Pedagogical eradication of VSEPR/rabbit-ear trappings is thus a win–win situation, both for the freshman-level course as well as the advanced courses that aim to bring students toward the frontiers of current chemical research.

## Appendix 1: critique of the purported “unitary equivalence” of conflicting lone pair depictions

A version of the unitary invariance argument for inequivalent and equivalent lone pairs is presented in the recent monograph of Shaik and Hiberty (2008, pp. 107–109) which may be taken as

representative. In this argument, equivalent rabbit-ear hybrids  $h_r$ ,  $h_r'$  are expressed (in unnormalized form) by proportionality relations of the form

$$h_r \propto n + \lambda p \quad (\text{A.1a})$$

$$h_r' \propto n - \lambda p \quad (\text{A.1b})$$

where  $p = p_y$  (perpendicular to the molecular plane),  $n$  is an in-plane  $sp^n$ -type hybrid, and  $\lambda$  is a mixing parameter (left unspecified in their discussion). Visually (*cf.* Scheme 5.3 of the Shaik–Hiberty discussion), such mixtures suggest a superficial resemblance to  $sp^3$  hybrids. However, only  $\lambda = 1$  is allowed by Fock's theorem, because the transformation is otherwise non-unitary and  $h_r$ ,  $h_r'$  become nonorthogonal. The envisioned orthonormal rabbit-ears hybrids must therefore be expressed more explicitly as

$$h_r = 2^{-1/2}(n + p) \quad (\text{A.2a})$$

$$h_r' = 2^{-1/2}(n - p) \quad (\text{A.2b})$$

with associated orbital energies

$$\varepsilon_r = (\varepsilon_n + \varepsilon_p + 2F_{np})/2 \quad (\text{A.3a})$$

$$\varepsilon_r' = (\varepsilon_n + \varepsilon_p - 2F_{np})/2 \quad (\text{A.3b})$$

These orbitals are indeed equivalent ( $\varepsilon_r = \varepsilon_r'$ ), because off-diagonal  $F_{n,p} = \langle n|F|p \rangle$  matrix elements between MOs are vanishing.

However, the transformed orbitals  $h_r$ ,  $h_r'$  are generally not “ $sp^3$  hybrids” and must exhibit rather strange energetic interactions. If we assume, *e.g.*, that  $n$  is an  $sp^2$  hybrid along the  $z$  axis

$$n = 3^{-1/2}(s + 2^{1/2}p_z) \quad (\text{A.4})$$

then  $h_r$ ,  $h_r'$  become explicitly

$$h_r = 6^{-1/2}[s + 3^{1/2}p_y + 2^{1/2}p_z] \quad (\text{A.5a})$$

$$h_r' = 6^{-1/2}[s - 3^{1/2}p_y + 2^{1/2}p_z] \quad (\text{A.5b})$$

neither of which (83%  $p$ -character) is of idealized  $sp^3$  form. Moreover, these orbitals have the surprising Fock matrix interaction element

$$F_{r,r'} = \langle h_r|F|h_r' \rangle = 1/2\langle n + p|F|n - p \rangle = (\varepsilon_n - \varepsilon_p)/2 \quad (\text{A.6})$$

even though  $\langle h_r|h_r' \rangle = 0$ ! For water (B3LYP/6-311++G\*\* level), this interaction evaluates to an alarmingly large value

$$F_{r,r'} = -108 \text{ kcal mol}^{-1} \quad (\text{A.7})$$

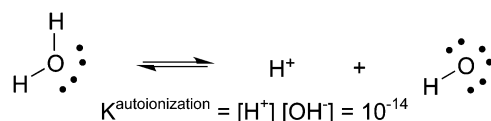
which could not be considered “ignorable” except in the context of a crude Hückel-like model (with the assumption  $F_{r,r'} = k\langle h_r|h_r' \rangle = 0$ , *perforce* vanishing). In this limit, the lone pairs must also be implicitly assumed to be degenerate in energy ( $\varepsilon_n = \varepsilon_p$ ), in conflict with spectroscopic properties such as first recognized by Zimmerman (1963). Thus, the supposed “equivalence” of  $(n,p)$  vs.  $(h_r,h_r')$  lone pairs rests on approximations that are unacceptable by current standards of accuracy.

## Appendix 2: a sample freshman-level handout on donor–acceptor interactions

### Bonding and Donor–Acceptor Concepts, Chem 104, Prof. Landis

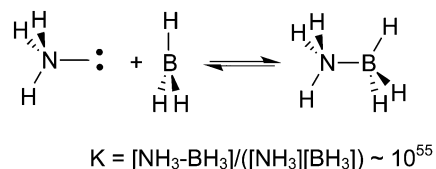
Chemistry presents a bewildering array of transformations: acid–base reactions, doping of semiconductors, transfer of electrons in oxidation and reduction reactions, condensation/hydrolysis pairs, substitution reactions, formation of hydrogen bonds, and so on. Rather than memorizing thousands of reactions it is helpful to think about *how* they occur using the concept of donor–acceptor interactions. This unifying concept provides a deep framework that reveals the underlying kinships amongst seemingly unrelated reactions.

*An acceptor is an atom, molecule, ion, or even solid-state material that has vacant orbitals to which electrons can be donated. A donor is an atom, molecule, ion, or material that has loosely held electrons that can be donated to an acceptor.* To illustrate the donor/acceptor concept consider the following representation of the autoionization equilibrium of water (*N.B.*, this representation does *not* show the other water molecules that interact with the reactants and products in bulk liquid water).



Focus on the *right-to-left* (reverse) reaction direction. The  $H^+$  ion is a hydrogen atom with no electrons in its valence  $1s$  shell – *i.e.*, a bare proton. The presence of an empty valence  $1s$  orbital makes  $H^+$  an electron pair acceptor. The  $OH^-$  ion has three lone pairs in its valence shell that can be donated to an empty orbital. From the donor–acceptor perspective, the formation of the O–H bond of water is the result of a strong donor,  $OH^-$ , donating an electron pair to a strong acceptor,  $H^+$ , to make an electron-pair covalent bond. The equilibrium lies to the left, as might be expected when a strong donor ( $OH^-$ ) and acceptor ( $H^+$ ) are allowed to react.

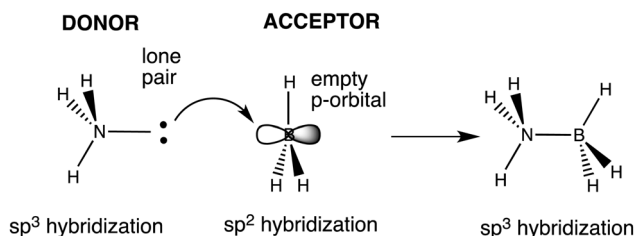
Consider another example that you may have seen in previous chemistry courses: the reaction of ammonia with borane to make the Lewis acid–base adduct.



The formation of  $H_3N-BH_3$  from ammonia and borane is very favorable (the equilibrium constant is estimated to be very large), suggesting that ammonia is a good donor and  $BH_3$  is a good acceptor. To better understand the acceptor properties of

BH<sub>3</sub> we need to first consider the bonding in BH<sub>3</sub> using a localized bond (aka valence bond) approach.

The B ground state electron configuration is [He]2s<sup>2</sup>2p<sup>1</sup>. Therefore, there are three valence electrons and four valence atomic orbitals, one 2s and the three 2p orbitals, available to make bonds. In BH<sub>3</sub> the three B–H bonds have sp<sup>2</sup> hybridization, meaning that two p-orbitals and one s-orbital were mixed together in making three equivalent sp<sup>2</sup> hybrids. These orbitals all lie in the same plane, yielding a trigonal planar geometry with 120° bond angles. But only *two* of the *three* p-orbitals in the valence shell of B were used to make the B–H bonds. This means that one p-orbital is vacant; it lies perpendicular to the plane of B and H atoms. The vacant p-orbital of B is an electron pair acceptor.



Now look at the Lewis structure for NH<sub>3</sub>. You should be able to devise the following descriptors: approximately sp<sup>3</sup> hybridization of the N atom, three N–H bonds, one lone pair, and a trigonal pyramidal molecular structure. The lone pair is a potential donor. When an ammonia molecule and a borane

molecule come close to one another, the lone pair on N can be donated into the empty p-orbital on B to create a donor–acceptor interaction. We symbolize this donor–acceptor interaction with a *curved arrow*. This donor–acceptor interaction increases as the two molecules come closer together, ultimately resulting in a N–B bond. The increase in bond number at B forces the hybridization to change from sp<sup>2</sup> to sp<sup>3</sup>, and the final H<sub>3</sub>N–BH<sub>3</sub> molecule has a tetrahedral arrangement of bonds.

### Strengths of donors and acceptors

In the previous example we emphasized that *any* lone pair is a potential donor. But not all lone pairs are equally good donors. Engagement in a donor–acceptor interaction requires that the donor electron pair shift from being localized solely on one atom to being shared with the acceptor. This suggests that the *more tightly a donor lone pair is localized on the atom, the poorer its donor ability*. As a result, charge and electronegativity strongly affect the donor strength of a lone pair.

Consider the three examples of functional groups with lone pairs: methylamine, methanol, and fluoromethane. The order of electronegativity is F > O > N. Electronegativity represents the tendency of an atom to draw electrons toward itself when making a bond. In the context of making donor–acceptor bonds, we can expect electronegativity to correlate inversely with the donor ability of a lone pair. In other words, we expect the *lone pair donor strength to increase as N > O > F*.

### ConceptTest 78

How many lone pair donor atoms are present in the molecule below?

A. 1 donor  
B. 2 donors  
C. 3 donors  
D. 4 donors  
E. 5 donors

Landis Chem 104 2014 Spring 205

### ConceptTest 78 Answer

How many lone pair donor atoms are present in the molecule below?

A. 1 donor  
B. 2 donors  
C. 3 donors  
D. 4 donors ★  
E. 5 donors

Landis Chem 104 2014 Spring 206

### ConceptTest 79

Which donor atom is expected to be the strongest donor?

A. -NR<sub>2</sub>  
B. OR<sub>2</sub>  
C. NR<sub>3</sub>  
D. FR

Landis Chem 104 2014 Spring 1

### ConceptTest 79 Answer

Which donor atom is expected to be the strongest donor?

A. -NR<sub>2</sub> ★ Donor Order  
B. OR<sub>2</sub> Anionic N > neutral N > O > F  
C. NR<sub>3</sub>  
D. FR Anion > Neutral  
Donor Strength decreases with increasing EN

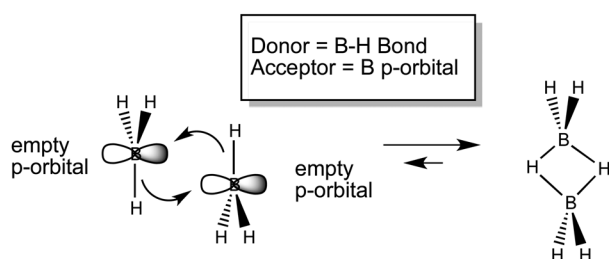
Landis Chem 104 2014 Spring 208

Charge, also, affects donor ability. Consider a neutral amine ( $\text{NH}_3$ ) and an amide anion ( $\text{NH}_2^-$ ). The anion has an excess of negative charge, making the electron pairs easier to donate than the more tightly held lone pair of the neutral atom. Thus, as the *negative charge of a donor atom increases, the donor strength increases*. Therefore we expect the donor abilities of neutral and anionic N, O, and F lone pairs to exhibit the trend  $\text{NH}_2^- > \text{NH}_3$ ;  $\text{OH}^- > \text{OH}_2$ ;  $\text{F}^- > \text{F-H}$ .

We can use similar reasoning to rationalize the relative *acceptor* abilities of atoms with vacant valence orbitals. The molecule  $\text{BH}_3$  is isoelectronic with the molecular cation  $^+\text{CH}_3$  (called the methyl carbenium ion). Analogously with  $\text{BH}_3$ , the methyl cation has a trigonal planar structure with an empty p-orbital lying perpendicular to the molecular plane and three C-H bonds made from C  $\text{sp}^2$  hybrid orbitals lying in the plane. However the positive charge of  $^+\text{CH}_3$  makes it a much stronger acceptor than neutral  $\text{BH}_3$ . As the electron pair of a donor moves closer to the  $^+\text{CH}_3$  acceptor, it feels the strong attraction of a positive charge that is absent in the case of neutral  $\text{BH}_3$ . Similar reasoning suggests that the more electronegative the acceptor atom, the stronger the acceptor character. Therefore we expect the acceptor strengths to follow trends like:  $^+\text{CH}_3 > ^+\text{SiH}_3$  and  $^+\text{CH}_3 > \text{BH}_3$ .

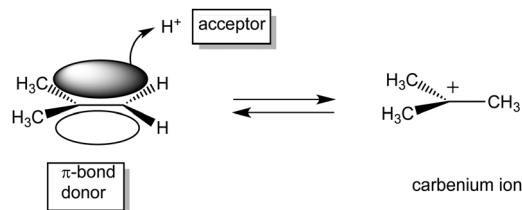
### Donors and acceptors beyond lone pairs and empty valence atomic orbitals

Electron pairs of bonds, also, can engage in donor-acceptor interactions. For example, free  $\text{BH}_3$  molecules are rarely observed; instead the dimer,  $\text{B}_2\text{H}_6$ , is the common form of this compound. As described above,  $\text{BH}_3$  is a good acceptor because it has an empty valence p-orbital on boron. When two  $\text{BH}_3$  molecules approach one another, the B-H bond pairs can act as donors with B-H pair of each molecule donated into the empty p-orbital of the other. In general, electron pairs in bonds are weaker donors than lone pairs of electrons.

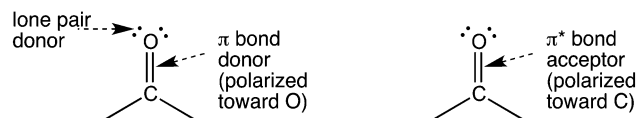


The C-C multiple bonds of unsaturated organic molecules have both  $\sigma$ - and  $\pi$ -bonding electron pairs. The  $\pi$ -bonds are weaker than the  $\sigma$ -bonds, implying that  $\pi$ -bonds are potential donors. A prototypical reaction of this type is the reaction of isobutene with an  $\text{H}^+$  to form a carbenium ion. The  $\pi$ -bond is the donor and  $\text{H}^+$  is the acceptor. The product carbenium ion is itself a strong acceptor. Therefore, when scanning a molecule for potential donor sites, pay attention to  $\pi$ -bonds also; be on the lookout for alkenes, alkynes, and molecules with C=O bonds (aldehydes, ketones, esters, *etc.*) or C=N  $\pi$ -bonds (nitriles, imines, *etc.*). The  $\pi$ -bond, like other bond electron

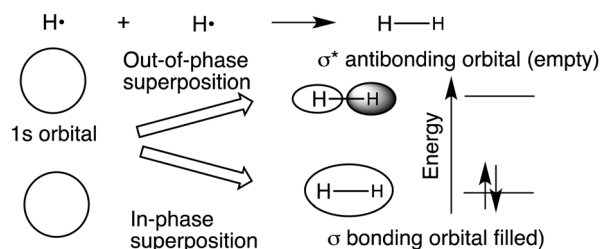
pairs, is not a strong donor in the thermodynamic sense (*vide infra*) but can be important kinetically.



Molecules with C=O functional groups are called carbonyls. Note that one could consider both the C=O  $\pi$ -bond and the lone pairs on the oxygen atoms as potential donor groups.



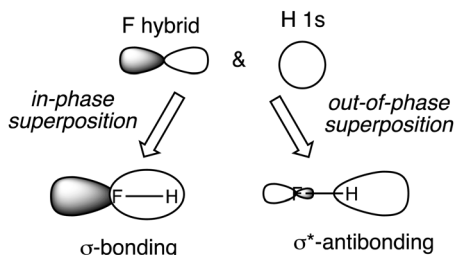
Although it may seem strange, antibonding orbitals can serve as electron pair acceptors. Let's first review what we mean by an antibonding orbital. When two singly occupied orbitals, such as the 1s orbitals of two H atoms, come close in space the quantum principle of superposition dictates that two molecular orbitals are formed. One superposition has "in-phase" character and results in accumulation of electron density between the two nuclei. This new orbital is called a *bonding* orbital, because it results in a lower enthalpy of the bonded atoms relative to the separated atoms. The other superposition has "out-of-phase" character and results in a depletion of electron density between the two nuclei. Placing electrons in the "out-of-phase" superposition does NOT lower the enthalpy of the bonded atoms relative to the separate atoms. Therefore, the "out-of-phase" superposition is called an *antibonding* orbital. Antibonding orbitals are designated by a \* as  $\sigma^*$  for a sigma antibond and  $\pi^*$  for a pi antibond.



For two atoms that are bonded together, the bonding orbital is filled with a pair of electrons and lies lower in energy than the unfilled antibonding orbital. What you should remember is that every time a filled bonding orbital is created an unfilled antibonding orbital is made: "*for every bond, an antibond*".

Antibonding orbitals are more than mathematical curiosities. An *antibond* is an unfilled orbital that can accept a pair of electrons. In particular, the antibonding orbitals associated with weak or highly polar bonds are good acceptors. For example, the C-C  $\pi$  bonds of hydrocarbons are weaker than the  $\sigma$ -bonds. Correspondingly, the C-C  $\pi^*$  orbitals are better acceptors than C-C or C-H  $\sigma^*$  orbitals (you can rationalize this by considering relative orbital energies; in a weak bond the bonding orbitals are higher in energy and weak bonds are lower in energy relative to a strong bond).

When a  $\sigma$ - or  $\pi$ -bond is formed between atoms of different electronegativity, such as hydrogen fluoride, the filled bonding orbital is *polarized* toward the more electronegative atom. In other words the electrons are distributed unequally with the more electronegative atom getting more than its “share”. Accurate quantum mechanical computations reveal the shared electron pair of HF is 80% associated with the F atom and only 20% associated with the H atom – hardly equal sharing.



According to the principle of superposition, if the bonding orbital is polarized toward the more electronegative atom, the antibonding orbital is polarized toward the less electronegative atom. In the graphic depiction above, the polarization of the antibonding orbital toward H is shown by the “fatter” H component and the “shrunk” F part. Quantum mechanical calculations show the H-F  $\sigma^*$  antibonding orbital to have 80% contribution from H and 20% from F. Orbital polarization means that donor–acceptor interactions with  $\sigma^*$  or  $\pi^*$  antibonds will be strongest when the donor comes close to the less electronegative atom of the bonded pair. The less electronegative atom will tend to have greater partial positive charge, which also will favor interaction with the incoming donor electrons.

Consider a simple example before we go on to more complex reactions: hydrogen bonding in solid HF. Two HF molecules can form a hydrogen bonded “super molecule” or chain through the donation of a F lone pair of one HF molecule into the  $\sigma^*$  orbital of another HF molecule.

Common donors

Lone pairs: C, N, O, P, S, Halogens  
 $\pi$  bonds: C=C, C=O, C=N, and C $\equiv$ C  
 $\sigma$  bonds: C-Li, C-Mg, C-Zn, H-B

Common acceptors

Empty valence orbitals: H<sup>+</sup>, carbenium ions, trivalent B & Al  
 $\pi^*$  orbitals: C=C, C=O, and C=N  
 $\sigma^*$  orbitals: H-halogen, H-O, H-N, C-halogen, C-O

Whether a strong donor–acceptor interaction will occur depends on **both** the donor and acceptor. In general the C=C  $\pi$ -bond is a modest donor, but H<sup>+</sup> is a strong acceptor. Therefore, the  $\pi$ -bond-to-H<sup>+</sup> donor–acceptor interaction can lead to formation of a carbenium ion in at least low equilibrium concentrations. We might not expect a significant donor–acceptor interaction at all for an alkene interacting with a substantially weaker acceptor than H<sup>+</sup>.

For those that go on to take organic chemistry, many instances of reactions that involve reactant donor–acceptor interactions will be seen. We focus here on the acid catalyzed conversion of an alcohol and isobutene to an ether.

Arrows: curved, straight, and double-headed

We need to be very particular about how we use arrows in Chemistry. In Chemistry 104 the following definitions and uses will be followed rigorously.

(1) Straight arrows with one arrow-head in either forward or reverse or both directions: are chemical reaction arrows and indicate the *rearrangement of atom positions and bonds* in going from reactant to products.



(2) Curved arrows indicate donor–acceptor interactions of electrons and vacant orbitals changes in atom positions are

**ConcepTest 81**  
 How many potential *acceptor sites* does this molecule have?

A. One  
 B. Two  
 C. Three  
 D. Four  
 E. Five

**ConcepTest 81 Answer**  
 How many potential *acceptor sites* does this molecule have?

A. One  
 B. Two  
 C. Three ★  
 D. Four  
 E. Five

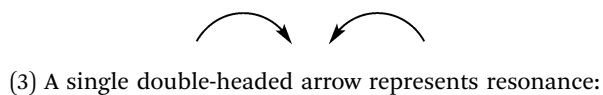
**ConcepTest 80**  
 Hydrogen bonding in H<sub>2</sub>X molecules is the result of strong donor–acceptor interactions between X lone pairs and H-X  $\sigma^*$  antibonds. Based on this description which of the structures below is expected for solid HF?

A. [Linear chain of HF molecules with H...F...H...F...H...F...H]n  
 B. [Zigzag chain of HF molecules with H...F...H...F...H...F...H]n  
 C. [Zigzag chain of HF molecules with H...F...H...F...H...F...H]n

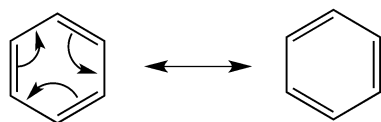
**ConcepTest 80 Answer**  
 Hydrogen bonding in H<sub>2</sub>X molecules is the result of strong donor–acceptor interactions between X lone pairs and H-X  $\sigma^*$  antibonds. Based on this description which of the structures below is expected for solid HF?

A. [Linear chain of HF molecules with H...F...H...F...H...F...H]n  
 B. [Zigzag chain of HF molecules with H...F...H...F...H...F...H]n  
 C. [Zigzag chain of HF molecules with H...F...H...F...H...F...H]n ★

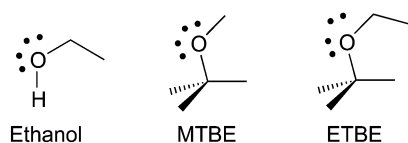
NOT implied by a curved arrow.



In resonance depictions all atoms are stationary, thus no chemical reaction is occurring. Resonance means that a single Lewis structure is insufficient to describe the distributions of electrons in a molecule. It is valid to use curved arrows to depict the donor-acceptor interactions that transform one Lewis structure into another. For the resonance in benzene the donors are the filled  $\pi$ -orbitals of one double bond and the acceptors are the unfilled  $\pi^*$  orbitals adjacent double bonds.

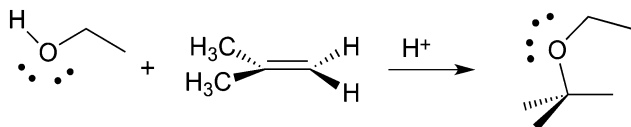


### Acid-catalyzed synthesis of ETBE from ethanol and isobutene

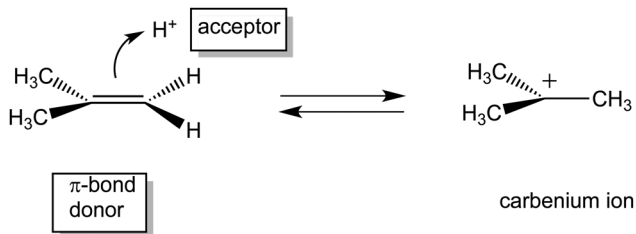


Reformulated gasolines (RFGs) have oxygenated additives such as ethanol, MTBE, and ETBE. Because these molecules already have oxygen incorporated in their structure, they enable car engines to operate with leaner air-to-fuel ratios than with pure hydrocarbon gasoline while achieving high combustion efficiency.

Commercially, ETBE is made by the reaction of ethanol and isobutene (also called 2-methylpropene) in the presence of an acid catalyst. In the absence of a catalyst, this reaction is very slow, too slow to make the quantities needed for reformulated gasoline. Our goal here is to see how the donor-acceptor paradigm provides insight into the nature of acid catalysis of the reaction between isobutene and ethanol.

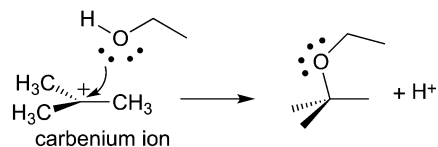


As we have already seen, the  $\pi$ -bond of an alkene can act as an electron pair donor and  $H^+$  is a good acceptor. This donor-acceptor interaction leads to the formation of a carbenium ion.



But the carbenium ion itself is a very strong acceptor and the oxygen lone pairs of ethanol are good donors. This suggests a

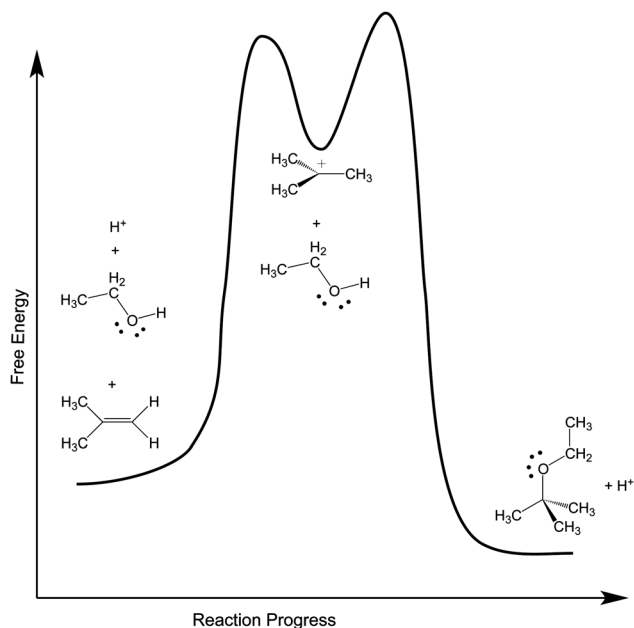
strong donor-acceptor interaction that ultimately leads to the product and regenerates the  $H^+$  catalyst by loss of  $H^+$  from the protonated ether oxygen. Remember that, by definition, a catalyst must not be consumed or created in the overall reaction. This does not mean that the catalyst is not involved in bond-making and breaking as the reaction progresses – as we have seen  $H^+$  is intimately involved in reacting with isobutene. Rather, catalysis requires that the reaction of  $H^+$  in the first step must be paired with a step in which the  $H^+$  is regenerated as a reaction product.

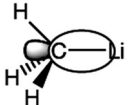
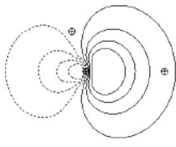
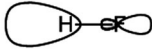
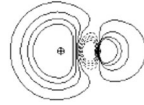
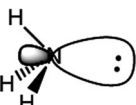
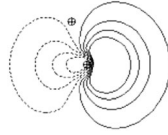

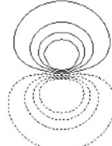
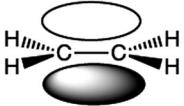
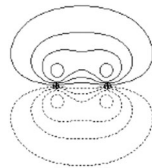
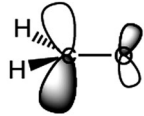
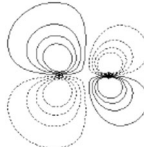


Acid-catalyzed formation of an ether from an alcohol and alkene is an example of a two-step reaction in which the carbenium ion is an intermediate. We can depict this overall transformation using a reaction coordinate diagram. Note that the intermediate carbenium ion is a shallow well on the free energy surface.

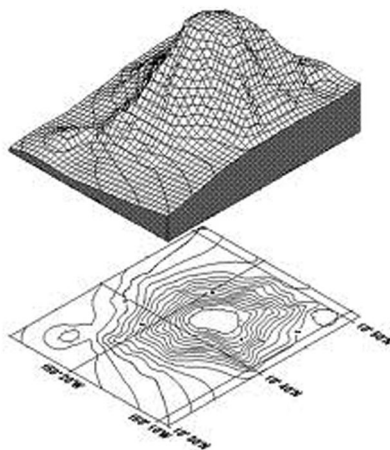
Also note from the reaction coordinate diagram that formation of a carbenium ion from  $H^+$  and an alkene is an energetically uphill process. From the change in free energy, one sees that the equilibrium constant for formation of a carbenium ion from alkene and  $H^+$  is small. Although the equilibrium lies far to the side of “alkene +  $H^+$ ”, the catalyst provides an overall lower free energy pathway to product than would occur in the absence of catalyst. This situation is common. Catalysts generally work by providing a reaction pathway that is *different and lower in activation energy* than non-catalyzed pathways. In this case the key effect of the catalyst is to generate a thermodynamically unstable but *highly reactive* carbenium ion.

Gallery of some donor and acceptor orbitals



Donor orbitals		Acceptor orbitals	
Cartoon drawing	Quantum calculation <sup>a</sup>	Cartoon drawing	Quantum calculation <sup>a</sup>
<p>H<sub>3</sub>C-Li</p>  <p>filled <math>\sigma</math> bond</p>		<p>H-F</p>  <p>empty <math>\sigma^*</math>-antibonding</p>	
<p>H<sub>3</sub>N</p>  <p>lone pair</p>		<p>CH<sub>3</sub><sup>+</sup></p>  <p>empty p-orbital</p>	
<p>H<sub>2</sub>C=CH<sub>2</sub></p>  <p>filled <math>\pi</math> bond</p>		<p>H<sub>2</sub>C=O</p>  <p>empty <math>\pi^*</math>-antibonding</p>	

<sup>a</sup>Quantum calculations demonstrate the orbitals as contour plots. You may have seen contours on terrain maps where the lines represent changes in elevation. In these contour maps the lines represent changes in the wavefunction (orbital) values. The dashed lines represent areas of negative phase and the solid lines are positive phase. Contour and relief of an island are shown below.



## References

- Alberts B., (2013), Prioritizing science education, *Science*, **340**, 249.
- Anet F. A. L. and Yavari I., (1977), Nitrogen inversion in piperidine, *J. Am. Chem. Soc.*, **99**, 2794–2796.
- Ansyn E. V. and Dougherty D., (2006), *Modern Physical Organic Chemistry*, Sausalito, CA: University Science Books, p. 102ff.
- Badenhoop J. and Weinhold F., (1997a), Natural bond orbital analysis of steric interactions, *J. Chem. Phys.*, **107**, 5406–5421.
- Badenhoop J. and Weinhold F., (1997b), Natural steric analysis: Ab initio van der Waals radii of atoms and ions, *J. Chem. Phys.*, **107**, 5422–5432.
- Badenhoop J. and Weinhold F., (1999), Natural steric analysis of internal rotation barriers, *Int. J. Quantum Chem.*, **72**, 269–280.
- Bader R. F. W., Henneker W. H. and Cade P. E., (1967), Molecular charge distributions and chemical binding, *J. Chem. Phys.*, **46**, 3341–3363.
- Beagley B. and McAloon K. T., (1971), Electron-diffraction study of the molecular structure of dimethyldisulphide, (CH<sub>3</sub>)<sub>2</sub>S<sub>2</sub>, *Trans. Faraday Soc.*, **67**, 3216–3222.
- Beagley B., Eckersley G. H., Brown D. P. and Tomlinson D., (1969), Molecular structure of S<sub>2</sub>Cl<sub>2</sub>, *Trans. Faraday Soc.*, **65**, 2300–2307.



- Bent H. A., (1961), An appraisal of valence-bond structures and hybridization in compounds of the first-row elements, *Chem. Rev.*, **61**, 275–311.
- Bickelhaupt F. M. and Baerends E. J., (2003), The case for steric repulsions causing the staggered conformation of ethane, *Angew. Chem., Int. Ed.*, **42**, 4183–4188.
- Carpenter J. E. and Weinhold F., (1988), Torsion-vibration interactions in hydrogen peroxide. 2. Natural bond orbital analysis, *J. Chem. Phys.*, **92**, 4306–4313.
- Clauss A. D. and Nelsen S. F., (2009), Integrating computational molecular modeling into the undergraduate organic chemistry curriculum, *J. Chem. Educ.*, **86**, 955–958.
- Coulson C. A., (1961), *Valence*, 2nd edn, London: Oxford, ch. 8.
- Delongchamps P., (1983), *Stereoelectronic Effects in Organic Chemistry*, Pergamon: Oxford.
- Fock V., (1930), Approximation methods for solution of the quantum mechanical many-body problem (*in German*), *Z. Physik*, **61**, 126–148.
- Foresman J. B. and Frisch A., (1996), *Exploring Chemistry with Electronic Structure Methods*, 2nd edn, Pittsburgh: Gaussian, Inc.
- Gillespie R. J., (1963), The valence-shell electron-pair repulsion (VSEPR) theory of directed valency, *J. Chem. Educ.*, **40**, 295–301.
- Gillespie R. J., (1974), A defense of the valence shell electron pair repulsion (VSEPR) model, *J. Chem. Educ.*, **51**, 367–370.
- Gillespie R. J., (2004), Teaching molecular geometry with the VSEPR model, *J. Chem. Educ.*, **81**, 298–304.
- Gillespie R. J. and Nyholm R. S., (1957), Inorganic stereochemistry, *Quart. Rev.*, **11**, 339–380.
- Hahn J., Schmidt P., Reinartz K., Behrend J., Winnewisser G. and Yamada K. M. T., (1991), Synthesis and molecular structure of disulfane, *Z. Naturforsch.*, **46b**, 1338–1342.
- Hinze S. R., Rapp D. N., Williamson V. M., Shultz M. J. Deslongchamps G. and Williamson K. C., (2013), Beyond ball-and-stick: students' processing of novel STEM visualizations, *Learn. Instr.*, **26**, 12–21.
- Jones R. A. Y., Katritzky A. R., Saba S. and Sparrow A. J., (1974), The conformational analysis of saturated heterocycles. Part LXIII. Tetrahydro-1,2 oxazines and related acyclic hydroxylamines, *J. Chem. Soc., Perkin Trans. 2*, 1554–1557.
- Jorgensen W. L. and Salem L., (1973), *The Organic Chemist's Book of Orbitals*, New York: Academic, p. 42.
- Katritzky A. R. and Lagowski J. M., (1967), *Principles of Heterocyclic Chemistry*, London: Methuen, p. 144ff.
- Kirby A. J., (1983), *The Anomeric Effect and Related Stereoelectronic Effects at Oxygen*, New York: Springer.
- Kniep R., Korte L. and Mootz D., (1983), Crystal Structures of Compounds  $A_2X_2$  ( $A = S, Se, X = Cl, Br$ ) (*in German*), *Z. Naturforsch.*, **38b**, 1–6.
- Kuczowski R. L., (1964), The mass and microwave spectra, structures, and dipole moments of the isomers of sulfur monofluoride, *J. Am. Chem. Soc.*, **86**, 3617–3621.
- Laing M., (1987), No rabbit ears on water. The structure of the water molecule: What should we tell the students? *J. Chem. Educ.*, **64**, 124–129.
- Levy Nahum T., Mamlok-Naaman R, Hofstein A. and Kronik L., (2008), A new “bottom-up” framework for teaching chemical bonding, *J. Chem. Educ.*, **85**, 1680–1685.
- Marsden C. J., Oberhammer H., Lösing O. and Willner H., (1989), The geometric structures of the disulphur difluoride isomers: an experimental and ab initio study, *J. Mol. Struct.*, **193**, 233–245.
- Moore J. W. and Stanitski C. L., (2015), *Chemistry: The Molecular Science*, 5th edn, Stamford, CT: Cengage Learning.
- Nelsen S. F., Thompson-Colon J. A., Kirste B., Rosenhouse A. and Kaftory M., (1987), One-electron oxidation of 3-substituted 2-oxa-3-azabicyclo-[2,2,2]octane derivatives, *J. Am. Chem. Soc.*, **109**, 7128–7136.
- Pauling L., (1931), The nature of the chemical bond. Application of results obtained from the quantum mechanics and from a theory of paramagnetic susceptibility to the structure of molecules, *J. Am. Chem. Soc.*, **53**, 1367–1400.
- Petillo P. A. and Lerner L. E., (1993), Origin and quantitative modeling of anomeric effect, in Thatcher G. R. J. (ed.), *The Anomeric Effect and Related Stereoelectronic Effects*, Washington: American Chemical Society, ch. 9.
- Pophristic V. and Goodman L., (2001), Hyperconjugation not steric repulsion leads to the staggered structure of ethane, *Nature*, **411**, 565–568.
- Reed A. E. and Weinhold F., (1985), Natural localized molecular orbitals, *J. Chem. Phys.*, **83**, 1736–1740.
- Riddell F. G., (1981), The conformations of hydroxylamine derivatives, *Tetrahedron*, **37**, 849–858.
- Schreiner P. R., (2002), Teaching the right reasons: lessons from the mistaken origin of the rotational barrier in ethane, *Angew. Chem., Int. Ed.*, **41**, 3579–3582.
- Shaik S. and Hiberty P. C., (2008), *A Chemist's Guide to Valence Bond Theory*, Hoboken, NJ: Wiley-Interscience.
- Slater J. C., (1931), Directed valence in polyatomic molecules, *Phys. Rev.*, **37**, 481–489.
- Studel R., (1975), Properties of sulfur-sulfur bonds, *Angew. Chem., Int. Ed. Engl.*, **14**, 655–664.
- Streitwieser, Jr. A., (1961), *Molecular Orbital Theory for Organic Chemists*, New York: Wiley.
- Sutter D., Dreizler H. and Rudolph H. D., (1965), Microwave spectrum, structure, dipole moment, and rotation barrier potential of dimethyldisulfide, *Z. Naturforsch.*, **20a**, 1676–1681 (*in German*).
- Walsh A. D., (1953), The electronic orbitals, shapes, and spectra of polyatomic molecules, *J. Chem. Soc. London*, 2260–2331.
- Weinhold F., (1999), Chemical bonding as a superposition phenomenon, *J. Chem. Educ.*, **76**, 1141–1146.
- Weinhold F., (2003), Rebuttal to the Bickelhaupt–Baerends case for steric repulsion causing the staggered conformation of ethane, *Angew. Chem., Int. Ed.*, **42**, 4188–4194.
- Weinhold F., (2012), Natural bond orbital analysis: A critical overview of its relationship to alternative bonding perspectives, *J. Comp. Chem.*, **33**, 2363–2379.
- Weinhold F. and Klein R. A., (2014), What is a hydrogen bond? Resonance covalency in the supramolecular domain, *Chem. Educ. Res. Pract.*, DOI: 10.1039/C4RP00030G.
- Weinhold F. and Landis C. R., (2001), Natural bond orbitals and extensions of localized bonding concepts, *Chem. Educ. Res. Pract.*, **2**, 91–104.

- Weinhold F. and Landis C. R., (2005), *Valency and Bonding*, London: Cambridge U. Press.
- Weinhold F. and Landis C. R., (2012), *Discovering Chemistry with Natural Bond Orbitals*, Hoboken NJ: Wiley.
- Weisskopf V. W., (1975), Of atoms, mountains, and stars: a study in qualitative physics, *Science*, **187**, 605–612.
- Winnewisser G., Winnewisser M. and Gordy P. J., (1968), Millimeter-wave rotational spectrum of HSSH and DSSD. 1. Q branches, *J. Chem. Phys.*, **49**, 3465–3478.
- Yokozeki A. and Bauer S. H., (1976), Structures of dimethyl disulfide and methyl ethyl disulfide, determined by gas-phase electron diffraction. A vibrational analysis for mean square amplitudes, *J. Phys. Chem.*, **80**, 618–625.
- Zimmerman H. E., (1963), A new approach to mechanistic organic photochemistry, in Noyes W. A. Jr., Hammond, G. S. and Pitts, J. N. Jr. (ed.), *Advances in Photochemistry*, New York: Interscience, vol. 1, pp. 183–208.